Biochemical Pharmacology 78 (2009) 607–616

Contents lists available at ScienceDirect

Biochemical Pharmacology

journal homepage: www.elsevier.com/locate/biochempharm

Histamine H_4 receptor–RGS fusion proteins expressed in Sf9 insect cells: A sensitive and reliable approach for the functional characterization of histamine H_4 receptor ligands

Erich H. Schneider [a,*], Roland Seifert [b]

[a] University of Regensburg, Department of Pharmacology and Toxicology, Universitätsstr. 31, D-93053 Regensburg, Germany
[b] Institute of Pharmacology, Medical School of Hannover, Carl-Neuberg-Str. 1, D-30625 Hannover, Germany

ARTICLE INFO

Article history:
Received 6 April 2009
Accepted 11 May 2009

Keywords:
Histamine H_4 receptor
Fusion protein
RGS protein
Steady-state GTPase assay
Constitutive activity
G_i-proteins

ABSTRACT

The human histamine H_4 receptor (hH_4R), co-expressed with $G\alpha_{i2}$ and $G\beta_1\gamma_2$ in Sf9 cells, is highly constitutively active. In the steady-state GTPase assay, the full agonist histamine (HA) induces only a relatively small signal (~20–30%), resulting in a low signal-to background ratio. In order to improve this system for ligand screening purposes, the effects of the regulators of G-protein signaling (RGS) RGS4 and RGS19 (GAIP) were investigated. RGS4 and GAIP were fused to the C-terminus of hH_4R or co-expressed with non-fused hH_4R, always combined with $G\alpha_{i2}$ and $G\beta_1\gamma_2$. The non-fused RGS proteins did not significantly increase the relative effect of HA. With the hH_4R–RGS4 fusion protein the absolute GTPase activities, but not the relative HA-induced signal were increased. Fusion of hH_4R with GAIP caused a selective increase of the HA signal, resulting in an enhanced signal-to-noise ratio. A detailed characterization of the hH_4R–GAIP fusion protein (co-expressed with $G\alpha_{i2}$ and $G\beta_1\gamma_2$) and a comparison with the data obtained for the non-fused hH_4R (co-expressed with $G\alpha_{i2}$ and $G\beta_1\gamma_2$) led to the following results: (i) the relative agonist- and inverse agonist-induced signals at hH_4R–GAIP are markedly increased. (ii) Compared to the wild-type hH_4R, standard ligands show unaltered potencies and efficacies at hH_4R–GAIP. (iii) Like hH_4R, hH_4R–GAIP shows high and NaCl-resistant constitutive activity. (iv) hH_4R–GAIP shows the same G-protein selectivity profile as the non-fused hH_4R. Collectively, hH_4R–GAIP provides a sensitive test system for the characterization of hH_4R ligands and can replace the non-fused hH_4R in steady-state GTPase assays.

1. Introduction

Histamine exerts its physiological effects *via* binding at four different receptor subtypes. The H_1-receptor mediates e.g. the increase of vascular permeability and NO production associated with inflammatory and allergic reactions [1]. The H_2-receptor regulates gastric acid secretion and shows a positive inotropic effect on the heart [1]. The presynaptic H_3-receptor negatively modulates neurotransmitter release in the CNS [1]. The fourth histamine (HA) receptor was first pharmacologically characterized on human eosinophils [2] and was later identified as a GPCR with 390 amino acids [3], sharing 43% overall homology with the H_3-receptor [4].

The human histamine H_4 receptor (hH_4R) is expressed e.g. in spleen and bone marrow [5,6] and mediates HA-induced chemotaxis, e.g. of eosinophils [7] and mast cells [8], suggesting a role in inflammatory and immunological processes. Recently, the hH_4R was also detected in the brain and may be involved in the regulation of central neurotransmission [9].

In animal models, H_4R antagonists were effective in the treatment of itch [10], colitis [11] or allergic airway inflammation [12]. Since pruritus, colitis or asthma still lack a curative or at least an optimized alleviating therapy, it is vitally important to investigate the potential of hH_4R antagonists for the treatment of these widespread diseases. Thus, reliable test systems are required to characterize compounds that could serve as potential candidates for new hH_4R-antagonizing anti-inflammatory drugs. To obtain a most reliable readout of receptor activation or inhibition, it is necessary to determine the functional signal as proximal to the receptor activation event as possible. Assays that determine a signal more downstream from receptor activation (e.g. adenylyl cyclase or reporter gene assays), may suffer from unclear and complicated stoichiometry of the involved proteins or from interfering side-processes in the signal transduction cascade. For example, it is reported for S49 cells that G-proteins exist in stoichiometric excess compared to the effector adenylyl cyclase

* Corresponding author at: Department of Pharmacology and Toxicology, Institute of Pharmacy, University of Regensburg, Universitätsstr. 31, D-93053 Regensburg, Germany. Tel.: +49 941 4786; fax: +49 941 4772.
E-mail addresses: erich.schneider@chemie.uni-regensburg.de (E.H. Schneider), seifert.Roland@mh-hannover.de (R. Seifert).

0006-2952/$ – see front matter © 2009 Elsevier Inc. All rights reserved.
doi:10.1016/j.bcp.2009.05.015

(AC), which limits the agonist-induced stimulation of AC activity [13]. This may hamper the determination of small efficacy differences between different partial agonists in AC assays. Moreover, as reported for the hH_4R antagonist JNJ-7777120, cAMP reporter gene assays can eliminate the effects of partial inverse agonists, which, in contrast, are still detectable by steady-state GTPase assays [14].

The steady-state GTPase assay with receptors and G-proteins expressed in baculovirus-infected Sf9 cells provides a reliable and sensitive test system with a very proximal readout. In general, the steady-state GTPase assay, when used as readout for $G\alpha_i$-coupled receptors, shows a higher sensitivity than cAMP accumulation or AC assays [15]. When GPCR–$G\alpha$ fusion proteins are used, steady-state GTPase assays can be performed with a defined 1:1 stoichiometry of receptor and G-protein [16].

Steady-state GTPase assays with Sf9 cell membranes were successfully employed for the investigation of the formyl peptide receptor clone 26 [17], the chemokine receptor CXCR4 [18] or the cannabinoid receptor subtypes CB_1 and CB_2 [19]. Recently, we also reported on the characterization of the hH_4R in Sf9 cells [14]. However, the hH_4R system showed a very weak relative agonist-induced signal (20–30%). This resulted in a low signal-to-noise ratio. Fusion of the hH_4R to $G\alpha_{i2}$ did not improve the relative intensity of the agonist-induced signal, since it resulted in an increase of the constitutive activity in steady-state GTPase assays [14].

An interesting possibility to increase signal intensity in steady-state GTPase assays is the co-expression of regulators of G-protein signaling (RGS). RGS proteins form a large group of proteins that are classified in eight subfamilies, showing high structural diversity [20]. A common feature of all RGS proteins is the RGS-domain, which consists of 120 amino acids and is of central importance for binding $G\alpha$ subunits and accelerating their GTPase activity [20]. It has also been reported that the effect of RGS4 on the GTPase activity induced by the α_{2A} adrenoceptor was enhanced by fusing the C-terminus of the GPCR to the N-terminus of the RGS protein. Despite the covalent binding of the RGS protein to the receptor, there was no interference with receptor-mediated activation of the G-protein [21].

In this paper we report on the co-expression of the RGS proteins RGS4 and RGS19 (GAIP) with hH_4R, $G\alpha_{i2}$ and $G\beta_1\gamma_2$ in Sf9 cells by performing quadruple infections with genetically modified baculoviruses. Moreover, we adopted the approach from Ref. [21] to the H_4R and generated fusion proteins with RGS4 and GAIP that were co-expressed with $G\alpha_{i2}$ and $G\beta_1\gamma_2$.

RGS4 belongs to the R4 sub-family of RGS proteins and accelerates the GTPase activity of $G\alpha_i$ [22,23] and $G\alpha_q$ [24] proteins. Two conserved cysteines in the RGS4 N-terminus act as potential palmitoylation sites [25]. GAIP (RGS19) belongs to the RZ sub-family and interacts with members of the $G\alpha_i$ class, but not with $G\alpha_q$ [26]. Membrane-bound GAIP is highly palmitoylated in its cysteine string region, containing eight cysteines [26].

We chose these two RGS proteins, because they belong to the structurally simplest sub-families and do not possess additional functional domains. Their stimulating effect on GPCR-activated $G\alpha_q$ and $G\alpha_i$ proteins was previously demonstrated for the human H_1R [27] and the chemokine receptor CXCR4 [18]. Thus, RGS4 and GAIP should be promising candidates for enhancing the GTPase activity in the co-expression system of the hH_4R with $G\alpha_{i2}$ and $G\beta_1\gamma_2$.

2. Materials and methods

2.1. Materials

The pcDNA 3.1 plasmids containing the sequences encoding RGS4 and GAIP were obtained from the UMR cDNA Resource Center at the University of Missouri-Rolla (Rolla, MO, USA). The DNA primers for PCR were synthesized by MWG Biotech (Ebersberg, Germany). The *Pfu* polymerase was obtained from Stratagene (La Jolla, CA, USA). Restriction enzymes were purchased from New England Biolabs (Ipswich, MA, USA). Recombinant baculovirus encoding the unmodified versions of the $G\beta_1\gamma_2$ subunits was a kind gift of Dr. P. Gierschik (Department of Pharmacology and Toxicology, University of Ulm, Germany). Recombinant baculoviruses for $G\alpha_{i1}$, $G\alpha_{i2}$, and $G\alpha_{i3}$ were donated by Dr. A.G. Gilman (Department of Pharmacology, University of Southwestern Medical Center, Dallas, TX, USA) and the baculovirus encoding rat $G\alpha_o$ was generously provided by Dr. J.C. Garrison (University of Virginia, Charlottesville, VA). Baculoviruses for mammalian RGS4 and GAIP (N-terminally His-tagged) were kindly donated by Dr. E. Ross (Department of Pharmacology, University of Southwestern Medical Center, Dallas, TX, USA).

The anti-$G\alpha_o$ antibody was purchased from Calbiochem (San Diego, CA, USA); the M1 anti-FLAG antibody was obtained from Sigma (St. Louis, MO, USA). The antibody recognizing the $G\alpha_i$ subunits (anti-$G\alpha_{common}$) was generously provided by Dr. B. Nürnberg (Institute for Pharmacology, University of Tübingen, Germany). The antibodies selective for RGS4 and GAIP were purchased from Santa Cruz (Santa Cruz, CA, USA). The H_4R antagonist 1-[(5-chloro-1*H*-indol-2-yl)carbonyl]-4-methyl-piperazine (JNJ-7777120) was kindly provided by Dr. Robin Thurmond (Department of Immunology, Johnson & Johnson Pharmaceutical R&D, San Diego, CA, USA). Immepip, imetit, iodophenpropit, R-α-methylhistamine, 5-methylhistamine and THIO were obtained from Tocris (Avonmouth, Bristol, UK). HA was purchased from Sigma (St. Louis, MO, USA). The 10 mM stock solution of JNJ-7777120 was prepared in dry Me_2SO, the stock solutions (10 mM) and dilutions of all other H_4R agonists and antagonists described in this paper were prepared in distilled water.

[^{3}H]HA (specific activities 14–18 Ci/mmol) and [^{3}H]dihydroalprenolol (97.4 Ci/mmol) were obtained from PerkinElmer (Boston, MA, USA). [γ-^{32}P]GTP was purchased from PerkinElmer or was prepared in our laboratory using GDP and [^{32}P] (orthophosphoric acid, 150 mCi/ml, obtained from PerkinElmer) according to a previously described enzymatic labeling procedure [28]. $MgCl_2$ was purchased from Merck (Darmstadt, Germany) and Tris base was obtained from usb (Cleveland, OH, USA). Radioactive samples were counted in a PerkinElmer Tricarb 2800TR liquid scintillation analyzer.

2.2. Construction of pVL-1392 plasmids encoding FLAG-hH_4R-His_6, FLAG-hH_4R-His_6-$G\alpha_{i2}$, FLAG-hH_4R-His_6-RGS4 and FLAG-hH_4R-His_6-GAIP

The generation of FLAG-hH_4R-His_6 as well as of FLAG-hH_4R-His_6-$G\alpha_{i2}$ was previously described [14]. The hexahistidine tagged C-terminus of the histamine H_4 receptor was fused to the N-terminus of RGS4 or GAIP by overlap extension PCR using *Pfu* polymerase as follows.

For preparation of the FLAG-hH_4R-His_6-RGS4 fusion protein, two fusion primers were synthesized. The sense primer s6H-RGS4 (5′-CAC CAT CAT CAC CAT CAC ATG TGC AAA GGG CTT GC-3′) contained an 18 bp sequence encoding a hexahistidine tag followed by the first 17 bp of the RGS4 cDNA. The antisense primer a6H consisted only of the 18 bp sequence encoding the hexahistidine tag (5′-GTG ATG GTG ATG ATG GTG-3′). In PCR 1a the sequence between the sEcoRI-hH_4 primer (5′-GCC ATC ACA TCA TTC TTG GAA TTC GTG ATC CCA GTC-3′) and the a6H fusion primer was amplified using the pGEM-3Z-SF-hH_4R-His_6 plasmid as template. In PCR 1b the RGS4 sequence between the s6H-RGS4 fusion primer and the antisense primer aRGS4-XbaI (5′-TCT AGA CTC GAG TTA GGC ACA CTG AGG GAC C-3′) was

amplified using a pcDNA 3.1-RGS4 plasmid as template yielding a product with an extra XbaI site 3′ of the stop codon of RGS4. In PCR 2, the products of PCR 1a and 1b were used as templates together with the primers sEcoRI-hH_4 and aRGS4-XbaI. This resulted in a fragment encoding a part of the hH_4R, followed by a hexahistidine tag and the RGS4 sequence with an XbaI site 3′ of the stop codon. Since not only the hH_4R sequence, but also the RGS4 DNA contain an EcoRI site, it was not possible to use this site for cloning. Thus, the fragment obtained in PCR2 was digested with PshAI and XbaI and cloned into pGEM-3Z-SF-hH_4R-His_6 digested with the same enzymes to obtain the full-length fusion protein DNA sequence.

For preparation of the hH_4R–GAIP fusion protein, as fusion primers the sense primer s6H-GAIP (5′-CAC CAT CAT CAC CAT CAC ATG CCC ACC CCG CAT GAG-3′) containing an 18 bp sequence encoding a hexahistidine tag followed by the first 18 bp of the GAIP cDNA and the antisense primer a6H were used. PCR 1a was performed as described above for the generation of the hH_4R–RGS4 fusion protein. In PCR 1b the GAIP sequence between the s6H-GAIP fusion primer and an antisense primer aGAIP-XbaI (5′-TCT AGA CTC GAG CTA GGC CTC GGA GGA GG-3′) was amplified using a pcDNA 3.1-GAIP plasmid as template and yielding a product with an extra XbaI site 3′ of the stop codon of GAIP. In PCR 2 the products of PCR 1a and 1b were used as templates together with the primers sEcoRI-hH_4 and aGAIP-XbaI. This resulted in a fragment encoding a part of the hH_4R, followed by a hexahistidine tag and the GAIP sequence with an XbaI site 3′ of the stop codon. This fragment was digested with EcoRI and XbaI and cloned into pGEM-3Z-SF-hH_4R-His_6 digested with the same enzymes to obtain the full-length fusion protein DNA sequence.

PCR-generated DNA sequences were confirmed by the sequencing service of Entelechon (Regensburg, Germany). All fusion protein sequences were cloned into the baculovirus expression vector, pVL1392.

2.3. Generation of recombinant baculoviruses, cell culture and membrane preparation

Sf9 cells were cultured in 250 or 500 ml disposable Erlenmeyer flasks at 28 °C under rotation at 150 r.p.m. in SF 900 II medium (Invitrogen, Carlsbad, CA, USA) supplemented with 5% (v/v) fetal calf serum (Biochrom, Berlin, Germany) and 0.1 mg/ml gentamicin (Cambrex Bio Science, Walkersville, MD, USA). Cells were maintained at a density of 0.5–6.0 $\times$ 10^6 cells/ml. Recombinant baculoviruses were generated in Sf9 cells using the BaculoGOLD transfection kit (BDPharmingen, San Diego, CA, USA) according to the manufacturer's instructions. After initial transfection, high-titer virus stocks were generated by two sequential virus amplifications. The supernatant fluid from the second amplification was stored under light protection at 4 °C and used as routine virus stock for membrane preparations.

Infection of the cells with baculoviruses was performed as previously described [29]. The virus stocks were combined as described in Section 3. Sf9 membranes were prepared as described [30], using 1 mM EDTA (Merck, Darmstadt, Germany), 0.2 mM phenylmethylsulfonyl fluoride (Sigma, St. Louis, MO, USA), 10 μg/ml benzamidine (Sigma, St. Louis, MO, USA) and 10 μg/ml leupeptin (Calbiochem, San Diego, CA, USA) as protease inhibitors. Membranes were suspended in binding buffer (12.5 mM $MgCl_2$, 1 mM EDTA and 75 mM Tris/HCl, pH 7.4). All membrane preparations were stored at −80 °C until use.

2.4. [^{3}H]HA binding experiments

Prior to the experiments, membranes were sedimented by a 10 min centrifugation at 4 °C and 13,000 r.p.m. and resuspended in binding buffer (12.5 mM $MgCl_2$, 1 mM EDTA and 75 mM Tris/HCl, pH 7.4). For determination of B_{max} values, Sf9 membranes (75 μg per tube) were suspended in 250 μl of binding buffer supplemented with [^{3}H]HA (100 nM) and 0.2% (mass/vol.) bovine serum albumin (Sigma, St. Louis, MO, USA). Non-specific binding was determined in the presence of THIO (10 μM). Incubations were performed for 60 min at 25 °C and shaking at 250 r.p.m. Bound radioligand was separated from free radioligand by filtration through GF/C filters (Whatman, Maidstone, UK) pretreated with 0.3% (mass/vol.) polyethyleneimine (Sigma, St. Louis, MO, USA) and washed three times with 2 ml of ice-cold binding buffer (4 °C). Filter-bound radioactivity was determined by liquid scintillation counting.

2.5. Steady-state GTPase assay

Steady-state GTPase assays were essentially performed as previously described [29], but with 5.0 mM $MgCl_2$, 1.2 mM creatine phosphate (Sigma, St. Louis, MO, USA) and 1 μg of creatine kinase (Roche, Indianapolis, IN, USA) in the samples. The reaction temperature was 25–27 °C. If not indicated otherwise, each tube additionally contained 100 mM NaCl (Merck, Darmstadt, Germany). The samples for the determination of Gα enzyme kinetics were prepared with a higher amount of [γ-^{32}P]GTP (0.4–0.5 μCi/tube). Unlabelled GTP (Roche, Indianapolis, IN, USA) was added in increasing concentrations from 0 to 1500 nM. Due to the displacement of [γ-^{32}P]GTP from the Gα subunit, the signal-to-noise ratio of the GTPase signal is reduced by unlabeled GTP. Therefore, unlabeled GTP was not used at concentrations higher than 1.5 μM.

2.6. SDS-PAGE and immunoblot analysis

Membrane proteins were separated on SDS polyacrylamide gels containing 10% or 12% (mass/vol.) acrylamide (Sigma, St. Louis, MO, USA). Proteins were transferred onto Trans-Blot nitrocellulose membranes (Bio-Rad, Hercules, CA) and reacted with M1 anti-FLAG and anti-$G\alpha_o$ antibody solution (1:1000 each). The antibodies anti-$G\alpha_{common}$, anti-RGS4 and anti-GAIP were used in a 1:500 dilution. Protein bands were visualized by enhanced chemoluminescence (Pierce Chemical, Rockford, IL) using goat anti-mouse IgG (Sigma, St. Louis, MO, USA), donkey anti-rabbit IgG (GE Healthcare, Little Chalfont, Buckinghamshire, UK) or donkey anti goat IgG (Santa Cruz, CA, USA), all coupled to horseradish peroxidase. The expression level of proteins was roughly estimated by using appropriate dilutions of reference membranes expressing a defined level of FLAG-β_2AR protein. The FLAG-β_2AR expression level was determined by radioligand binding with [^{3}H]dihydroalprenolol ([^{3}H]DHA). Immunoblots were scanned with a GS-710 calibrated imaging densitometer (Bio-Rad, Hercules, CA, USA). The intensity of the bands was analyzed with the Quantity One 4.0.3 software (Bio-Rad, Hercules, CA, USA).

2.7. Miscellaneous

Protein concentrations were determined with the Bio-Rad DC protein assay kit. Saturation and competition experiments were analyzed by non-linear regression with the Prism 5.01 software (GraphPad, San Diego, CA, USA). All values are given as mean ± SD. If not stated otherwise, significance was always calculated using one-way ANOVA, followed by Dunnett's multiple comparison test (all columns *vs.* control column). For the discussion of the apparent K_m values in Section 3.4, one-way ANOVA was followed by Bonferronis' multiple comparison test (comparison of all pairs of columns). Significance was always defined as $p < 0.05$ (confidence interval 95%).

3. Results and discussion

3.1. Investigation of protein expression by immunoblotting

We co-expressed hH_4R, hH_4R–RGS4 and hH_4R–GAIP with $G\alpha_{i2}$ and $G\beta_1\gamma_2$ in Sf9 insect cells. Expression of the proteins was confirmed by immunoblotting. As shown in Fig. 1A, the M1 anti-FLAG antibody stained the hH_4R protein as well as the fusion proteins. The hH_4R signal consisted of three bands in the range between 37 and 44 kDa (Fig. 1A, lane 1). As previously reported [14,31], these multiple bands are due to receptor glycosylation, which most likely occurs at the potential glycosylation sites in the receptor N-terminus (Asn-5 and Asn-9). H_4R–RGS4 and H_4R–GAIP show also very broad and diffuse bands, indicating differently glycosylated species. The expression levels of hH_4R, hH_4R–RGS4 and hH_4R–GAIP were roughly assessed by comparison with a dilution series of a standard membrane expressing 7.5 pmol/mg FLAG-β_2AR. The B_{max} value of this reference membrane was determined by saturation binding with 10 nM of the β_2AR antagonist [^{3}H]dihydroalprenolol. We determined a B_{max} value of ~1.8 pmol/mg for hH_4R and an increased B_{max} value of ~3.1 and ~3.0 pmol/mg for hH_4R–RGS4 and hH_4R–GAIP (Fig. 1A). We also co-expressed hH_4R with $G\alpha_{i2}$, $G\beta_1\gamma_2$ and non-fused RGS4 or GAIP. In these membranes we detected RGS4 and GAIP with specific anti-RGS4 (Fig. 1B, left lane) and anti-GAIP antibodies (Fig. 1B, right lane), respectively. As expected, the molecular mass of GAIP was by about 0.5–1 kDa higher compared to RGS4. Moreover, GAIP formed a more diffuse band. This may be explained by a higher degree of palmitoylation, especially in the N-terminal cysteine string region, which is a characteristic feature of the RZ sub-family of RGS proteins [32].

3.2. Quantification of B_{max} values by radioligand binding with [^{3}H]HA

As shown in Fig. 1A, the quantification of receptor expression levels by immunoblotting showed increased B_{max} values for the hH_4R–RGS fusion proteins compared to the non-fused hH_4R. To confirm this difference, we also determined expression levels by radioligand binding experiments with [^{3}H]HA (100 nM). We determined 1.6 ± 0.4 and 1.7 ± 0.6 pmol/mg for hH_4R–RGS4 and hH_4R–GAIP, respectively, but a significantly ($p < 0.05$) lower expression of only 0.7 ± 0.1 pmol/mg for hH_4R in the standard co-expression system (mean ± SD, $n = 2$ in triplicates).

Interestingly, when the wild-type hH_4R was co-expressed with the non-fused RGS proteins (+$G\alpha_{i2}$ and $G\beta_1\gamma_2$), the B_{max} value was not significantly different from the expression level of hH_4R in the RGS protein-free standard co-expression system (hH_4R + $G\alpha_{i2}$ + $G\beta_1\gamma_2$). The B_{max} values were 0.7 ± 0.3 and 0.7 ± 0.1 pmol/mg for hH_4R in the presence of RGS4 and GAIP, respectively (mean ± SD, $n = 2$ in triplicates, membranes from two different preparations).

There are three possible explanations for the enhanced expression levels of the fusion proteins. First, fusion of RGS4 or GAIP to the hH_4R may lead to conformational stabilization of the hH_4R. The hH_4R was previously reported to be constitutively active and structurally instable [14]. Second, hH_4R–RGS fusion proteins may prevent the receptor protein from proteolytic degradation. Third, the fusion of RGS4 or GAIP to hH_4R may facilitate the formation of a signaling complex with $G\alpha_{i2}$. Such signaling complexes with participation of RGS proteins have been previously described [32,33]. Thus, RGS proteins incorporated in hH_4R–RGS fusion proteins may act as "scaffolding proteins" for the receptor–G-protein complex, leading to an imitation of an hH_4R–$G\alpha_{i2}$ fusion protein. A similar enhancing effect on the hH_4R expression level was previously reported for the fusion of hH_4R with $G\alpha_{i2}$ [14].

3.3. HA-stimulation, THIO-inhibition and baseline activity in the steady-state GTPase assay

We performed steady-state GTPase assays with all membranes in the presence of 100 nM of GTP (standard conditions) and determined the maximum stimulatory effect of the agonist HA

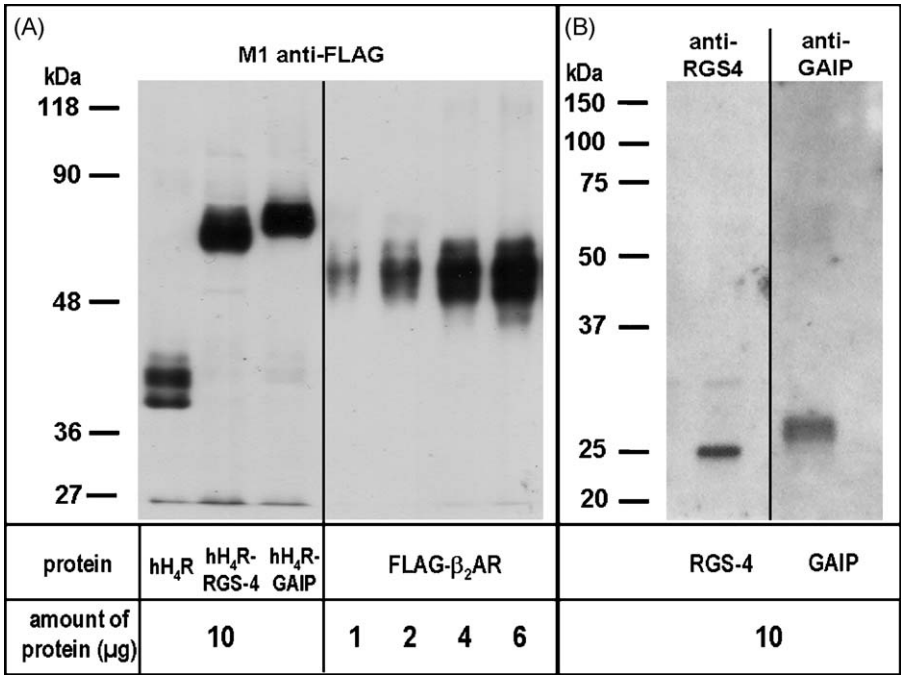

Fig. 1. Immunoblot analysis of hH_4R, hH_4R–RGS4, hH_4R–GAIP, RGS4 and GAIP in Sf9 cell membranes. Name and amount of the proteins loaded onto the gel are given below the lanes. (A) Detection of hH_4R, hH_4R–RGS4 and hH_4R–GAIP (all proteins FLAG-tagged) with the M1 monoclonal antibody (anti-FLAG Ig). Four dilutions of a reference membrane, expressing 7.5 pmol/mg FLAG-β_2AR and stained with the M1 antibody, were used for a rough estimation of protein expression levels (right part of panel A). The expression levels are 1.8 pmol/mg for wild-type hH_4R (lane 1), 3.1 pmol/mg for hH_4R–RGS4 (lane 2) and 3.0 pmol/mg for hH_4R–GAIP (lane 3). (B) Detection of non-fused RGS4 (left lane) and GAIP (right lane) with an anti-RGS4 and an anti-GAIP antibody, respectively. The numbers on the left of each panel indicate the molecular masses of the detected proteins in kDa. All immunoblots were performed as described under Section 2.

Table 1
Impact of RGS4 and GAIP (fused or co-expressed with hH_4R) on the baseline and on the relative effects of HA and THIO in the steady-state GTPase assay. The data were determined with membranes from Sf9 cells co-expressing the proteins given in the table with $G\alpha_{i2}$ and $G\beta_1\gamma_2$. All data are shown as mean ± SD (n given in the table). The results in the presence of RGS proteins were compared to the data obtained with the wild-type hH_4R in one-way ANOVA, followed by Dunnet's multiple comparison test (significant difference: $^{*}p < 0.05$, $^{**}p < 0.01$, $^{***}p < 0.001$). All experiments were performed in triplicates as described under Section 2.

Expressed proteins[a]	%Relative HA effect[b]	%Relative THIO effect[b]	%Increase of baseline[c]	Membranes[d]
Wild-type hH_4R	+31.8 ± 9.2 (n = 22)	−27.5 ± 11.3 (n = 20)	0.0 ± 44 (n = 23)	10
hH_4R–GAIP	+53.6 ± 16.4*** (n = 19)	−39.9 ± 7.0*** (n = 17)	+4.8 ± 38.2 (n = 20)	7
hH_4R + GAIP	+40.8 ± 12.3 (n = 7)	−37.3 ± 7.0 (n = 7)	−29.7 ± 34.4 (n = 8)	3
hH_4R–RGS4	+40.3 ± 14.1 (n = 9)	−40.9 ± 10.9** (n = 7)	+53.7 ± 59.6** (n = 10)	3
hH_4R + RGS4	+38.3 ± 12.9 (n = 9)	−39.2 ± 7.0** (n = 9)	−11.9 ± 34.3 (n = 10)	3

[a] Always expressed in combination with $G\alpha_{i2}$ and $G\beta_1\gamma_2$.
[b] %Change of absolute GTPase activity in the presence of ligand, related to baseline (control conditions), mean ± SD.
[c] Related to baseline of the standard system ($hH_4R + G\alpha_{i2} + G\beta_1\gamma_2$), mean ± SD.
[d] Number of different membranes (from different membrane preparations) used in the experiments.

(10 μM) and the maximum inhibitory effect of the inverse agonist THIO (10 μM). All results were compared to the properties of the standard co-expression system ($hH_4R + G\alpha_{i2} + G\beta_1\gamma_2$). When GAIP was co-expressed with hH_4R, $G\alpha_{i2}$ and $G\beta_1\gamma_2$, no significant alteration of the relative HA and THIO effects (related to baseline) and of the baseline activity was found (Table 1). RGS4, co-expressed with hH_4R, $G\alpha_{i2}$ and $G\beta_1\gamma_2$, significantly ($p < 0.01$, Table 1) increased the relative effect of THIO, but did not significantly influence the relative effect of HA and the baseline activity. The low or even lacking effect of RGS proteins co-expressed with hH_4R, $G\alpha_{i2}$ and $G\beta_1\gamma_2$ is surprising, since we previously found marked GTPase-stimulating effects of RGS proteins, when co-expressed with the chemokine receptor CXCR4, $G\alpha_{i2}$ and $G\beta_1\gamma_2$. Both RGS4 and GAIP increased the effect of the CXCR4 agonist SDF-1α (stroma-derived cell factor 1) in steady-state GTPase assays by ~50% [18]. Maybe, these different effects of RGS proteins co-expressed with hH_4R or CXCR4 are due to differing RGS–GPCR interactions. It is conceivable that the signaling complex consisting of the GPCR, the RGS protein and the heterotrimeric G-protein is not only stabilized by RGS–Gα interactions, but also by binding of the RGS protein to the GPCR. In fact, it was previously reported that the N-terminal domain of RGS4 interacts with G_q-coupled receptors, resulting in a receptor-selective inhibition of G-protein signaling [34].

The most pronounced effects were observed with the fusion proteins (Table 1). Compared to the standard co-expression system ($hH_4R + G\alpha_{i2} + G\beta_1\gamma_2$), there was a significant ($p < 0.01$) increase in baseline GTPase activity, when hH_4R–RGS4 was co-expressed with $G\alpha_{i2}$ and $G\beta_1\gamma_2$ (Table 1). Since hH_4R–RGS4 increased both the absolute constitutive GTPAse activity and the absolute HA-stimulated signal, there was no significant increase of the relative HA effect. Thus, this system shows no improved signal-to-noise ratio compared to the standard co-expression system (Table 1). However, hH_4R–RGS4 could be advantageous for the testing of inverse agonists, since a significant increase ($p < 0.01$) of the relative THIO effect was found (Table 1).

The most interesting results were found with the hH_4R–GAIP fusion protein (+$G\alpha_{i2}$ and $G\beta_1\gamma_2$). The hH_4R–GAIP fusion protein caused a significant ($p < 0.001$) increase of the relative HA and THIO effects. Surprisingly, compared to the RGS protein-free standard co-expression system ($hH_4R + G\alpha_{i2} + G\beta_1\gamma_2$), the relative stimulatory effect of HA was increased by ~70%. This was caused by a selective increase of agonist-stimulated absolute GTPase activity without a significant alteration of baseline GTPase activity.

This differential effect of RGS4 and GAIP could be due to a differing G-protein selectivity. RGS4 accelerates the GTPase activity of both G-protein families, $G\alpha_i$ [22,23] and $G\alpha_q$ [24]. By contrast, GAIP shows preference for $G\alpha_i$ proteins [25]. Interestingly, GAIP shows additional selectivity within the $G\alpha_i$ class. In the literature, a rather weak effect of GAIP on $G\alpha_{i2}$ was reported [26,35]. According to the UniProtKN/Swiss-Prot section of the UniProt knowledgebase [36] (entry P49795) GAIP binds to Gα proteins with the order of preference $G\alpha_{i3} > G\alpha_{i1} > G\alpha_o \gg G\alpha_{i2}$. Thus, the GAIP effect on $G\alpha_{i2}$ proteins may only become visible at very high concentrations of activated GTP-bound $G\alpha_{i2}$, e.g. when the system is activated by the agonist-stimulated hH_4R. By contrast, RGS4 shows a higher affinity for $G\alpha_{i2}$ and therefore the GTPase activating effect of RGS4 is already visible in the constitutively active system. This would explain why hH_4R–GAIP enhances selectively the HA-stimulated GTPase activity and therefore improves the signal-to-noise ratio. The hH_4R–RGS4 fusion protein, however, accelerates both constitutive and HA-stimulated GTPase activity and does not increase the relative HA signal.

Table 2
Effects of fused and co-expressed RGS proteins on $G\alpha_{i2}$ GTPase enzyme kinetics (V_{max} and apparent K_m values). "Apparent" K_m values were calculated after subtraction of the control curve from the enzyme kinetic curves representing the effects of HA and THIO (10 μM each). The resulting net curves were fitted according to a one-site binding function. The data are from the same experiments that were also used for the Eadie–Hofstee plots in Fig. 2. All data shown are mean ± SD (n given in the table) using membranes from at least two different batches. The results were compared using one-way ANOVA, followed by Bonferroni's multiple comparison test (K_m significantly different to: *wild-type hH_4R, $^{+}hH_4R$–$G\alpha_{i2}$, $^{\#}hH_4R$ + RGS4 or $^{\bullet}hH_4R$–GAIP, one symbol: $p < 0.05$, two symbols: $p < 0.01$, three symbols: $p < 0.001$). All experiments were performed in triplicates as described in Section 2.

Expressed proteins[a]	Range of V_{max}[b] [pmol/(min mg)]	App. K_m, agonist-stimulated (HA, 10 μM)[c] [nM]	App. K_m, inverse agonist-inhibited (THIO, 10 μM)[c] [nM]
hH_4R	6.0–27	462 ± 181 (n = 6)	379 ± 93 (n = 7)
hH_4R + RGS4	5.5–22	686 ± 104^{+++} (n = 5)	497 ± 100 (n = 5)
hH_4R + GAIP	4.4–20	882 ± 172$^{**,+++}$ (n = 3)	365 ± 38 (n = 3)
hH_4R–RGS4	15–58	970 ± 145$^{***,+++,\#,\bullet}$ (n = 7)	416 ± 86 (n = 5)
hH_4R–GAIP	11–39	697 ± 127^{+++} (n = 6)	350 ± 123 (n = 5)
hH_4R–$G\alpha_{i2}$	9.1–15	217 ± 76 (n = 4)	272 ± 133 (n = 4)

[a] Always expressed in combination with $G\alpha_{i2}$ and $G\beta_1\gamma_2$.
[b] V_{max} of the agonist-stimulated system (10 μM HA).
[c] Determined after normalizing the enzyme kinetic curves to V_{max} (10 μM HA) = 100% and subtraction of the control curve, mean ± SD.

3.4. Influence of RGS proteins on $G\alpha_{i2}$ enzyme kinetics (K_m and V_{max})

We investigated the GTPase enzyme kinetics of $G\alpha_{i2}$ by determination of steady-state GTPase activity in the presence of increasing concentrations of the substrate GTP. Due to the high inter-experimental and inter-membrane variability of absolute GTPase activities (cf. range of V_{max} given in Table 2) we normalized all enzyme kinetic curves to a range between 0% and 100%. The V_{max} of the HA-stimulated (10 μM) system (determined by non-linear regression) was set to 100%. After subtraction of the control curve (solvent) and fitting the curves according to a hyperbolic function (one-site binding), "apparent" K_m values were calculated, similarly to the calculation of K_d values previously reported for GTPγS saturation bindings [14,37]. The results are shown in Table 2.

To visualize the K_m effects of the RGS proteins, Eadie–Hofstee plots for every system are shown in Fig. 2. For these plots the normalized data (% of V_{max} in the presence of HA (10 μM), instead of absolute GTPase activity) were used without subtraction of the control curves. In Eadie–Hofstee plots the slope of the regression line represents $-K_m$. In the standard co-expression system the three linear regression lines representing THIO-inhibition, control conditions and HA-stimulation are in parallel, indicating that THIO and HA do not alter the K_m value of $G\alpha_{i2}$ in the absence of RGS proteins (Fig. 2A). However, when RGS4 or GAIP were co-expressed together with hH_4R (+$G\alpha_{i2}$ and $G\beta_1\gamma_2$), the slope of the regression line representing the HA-stimulated system was slightly increased, indicating an RGS-induced increase of the K_m value (Fig. 2C and D). This effect was also reported in the literature, where the addition of purified RGS4 to membranes expressing α_{2A}-adrenoceptor-Ile^{352}-$G\alpha_{i2}$ resulted in an increased K_m value, when the system was stimulated with the agonist UK-14304 (5-bromo-6-[2-imidazolin-2-ylamine]-quinoxaline) [23].

Despite the slightly increased slope of the HA-regression line in the Eadie–Hofstee plots, the apparent K_m value of the system co-expressing RGS4 with hH_4R, $G\alpha_{i2}$ and $G\beta_1\gamma_2$, was not significantly different from the RGS protein-free system. Only when GAIP was co-expressed with hH_4R, $G\alpha_{i2}$ and $G\beta_1\gamma_2$, the increase of the apparent K_m value reached significance (Table 2). Maybe, GAIP is more effectively integrated into the membrane *via* its palmitoylated cysteine string domain, which is not present in RGS4.

When RGS4 was fused to hH_4R (Fig. 2E, Table 2), the apparent K_m was significantly ($p < 0.05$) increased compared to the co-expression system with non-fused RGS4 (Fig. 2C, Table 2). This suggests that the fusion protein facilitates integration of RGS4 into the membrane and the formation of a signaling complex with $G\alpha_{i2}$. An increase of the Gα K_m value by a GPCR-RGS4 fusion protein was previously also shown for α_{2A}-adrenoceptor-RGS4, co-expressed with Cys351Ile $G\alpha_{o1}$, in the presence of the agonist UK-14304 [21].

By contrast, fusion of GAIP to hH_4R (hH_4R–GAIP) did not significantly alter the K_m value in comparison to non-fused GAIP (Table 2 and Fig. 2F) or to the RGS protein-free standard co-expression system (Table 2 and Fig. 2A). It is surprising that the hH_4R–GAIP fusion protein did not significantly increase the apparent K_m estimate under agonist stimulation, whereas either the H_4R + GAIP co-transfection or the H_4R–RGS4 fusion protein did. Maybe, when co-transfected with H_4R, the number of GAIP proteins located at the membrane is higher than in case of the hH_4R–GAIP fusion protein. When hH_4R–GAIP is expressed, the number of GAIP molecules at the membrane does never exceed the number of receptor molecules. However, when GAIP is co-transfected with H_4R, possibly more GAIP is recruited to the membrane, because it can be anchored in the membrane *via* the palmitoylated cysteine string motif [26]. By contrast, a large amount of co-transfected RGS4 may be located in the cytoplasm. RGS4 lacks a cysteine string motif and is recruited from a cytosolic pool mainly by interaction with membrane-associated G-proteins [38]. In our system, membrane localization of RGS4 may be increased, when hH_4R–RGS4 is expressed, since RGS4 is then anchored to the membrane by connection with the receptor protein. However, this is only speculation and it should also be considered that the non-significant increase of the agonist-stimulated K_m value in case of hH_4R–GAIP could only be caused by the high inter-experimental and inter-membrane variability of our data. Thus, these results should not be over-interpreted. A comparison of hH_4R–RGS4 with hH_4R–GAIP shows a significantly ($p < 0.05$) lower apparent K_m in the presence of hH_4R–GAIP. This may reflect the lower affinity of GAIP for $G\alpha_{i2}$, which was discussed in Section 3.3.

For comparison, in Fig. 2B also the Eadie–Hofstee plot for hH_4R–$G\alpha_{i2}$ co-expressed with $G\beta_1\gamma_2$ is shown. The data were taken from a previous publication [14]. Compared to the standard co-expression system (Fig. 2A), in case of hH_4R–$G\alpha_{i2}$ (Fig. 2B) the slope of all three regression lines is reduced, which is reflected by significantly lower apparent K_m values in Table 2. However, similarly to the standard co-expression system (Fig. 2A), also in the hH_4R–$G\alpha_{i2}$ fusion protein system all three regression lines are in parallel (Fig. 2B), as is expected in the absence of RGS proteins.

In the inverse agonist (THIO)-inhibited system, RGS4 and GAIP showed no significant effect on the K_m values, neither when fused to hH_4R nor when co-expressed with the receptor (Fig. 2 and Table 2).

3.5. Characterization of standard ligands at hH_4R, hH_4R–RGS4 and hH_4R–GAIP

As described above, co-expression of the hH_4R with RGS4 or GAIP did not result in a significant increase of the signal-to-noise ratio. By contrast, fusion of RGS4 or GAIP with hH_4R resulted in marked effects on absolute GTPase activities, with GAIP leading to a selective enhancement of the agonist-stimulated signal. Thus, the hH_4R–RGS fusion proteins are interesting candidates for a test system with improved sensitivity, compared to the standard co-expression system (hH_4R + $G\alpha_{i2}$ + $G\beta_1\gamma_2$).

In order to ensure that the pharmacological properties of hH_4R–RGS4 and hH_4R–GAIP are comparable with those of the wild-type hH_4R, we characterized several hH_4R standard ligands in the steady-state GTPase assay. In Table 3, the results from hH_4R–RGS4 and hH_4R–GAIP are compared with the data previously reported for the non-fused hH_4R [14]. In case of the hH_4R–GAIP fusion protein the EC_{50} values and efficacies did not significantly differ from the wild-type hH_4R data. However, significant differences were found for hH_4R–RGS4. 5-Methylhistamine, which showed an efficacy of 0.87 at the non-fused hH_4R is a full agonist (efficacy = 1.08) at the hH_4R–RGS4 fusion protein. The potencies of both HA and JNJ-7777120 were significantly reduced. The reduced potency of HA at the hH_4R–RGS4 fusion protein fits well to data from the literature [23]. It is reported that addition of purified RGS4 (100 nM) to membranes expressing the α_{2A}AR-Val^{351}-$G\alpha_{o1}$ fusion protein caused a more than 3-fold increase of the EC_{50} value of UK-14304 [23]. However, in our test system the expression level of hH_4R–RGS4 was only ~3 pmol/mg. This is more than 10,000-fold lower than the 100 nM of RGS4 that were added to the system in Ref. [23]. This explains the much weaker effect of RGS4 in our system, where the EC_{50} value of HA, was increased by only ~60%.

Taken together, our results show that the hH_4R–RGS fusion proteins maintain the pharmacology of the wild-type hH_4R to a large extent. Since the hH_4R–GAIP fusion protein, compared to the standard co-expression system (hH_4R + $G\alpha_{i2}$ + $G\beta_1\gamma_2$), resulted in an increased signal-to-noise ratio with unchanged ligand potencies and efficacies, we decided to use hH_4R–GAIP (+$G\alpha_{i2}$ + $G\beta_1\gamma_2$) as a standard test system for the characterization of hH_4R ligands in our medicinal chemistry program [39,40].

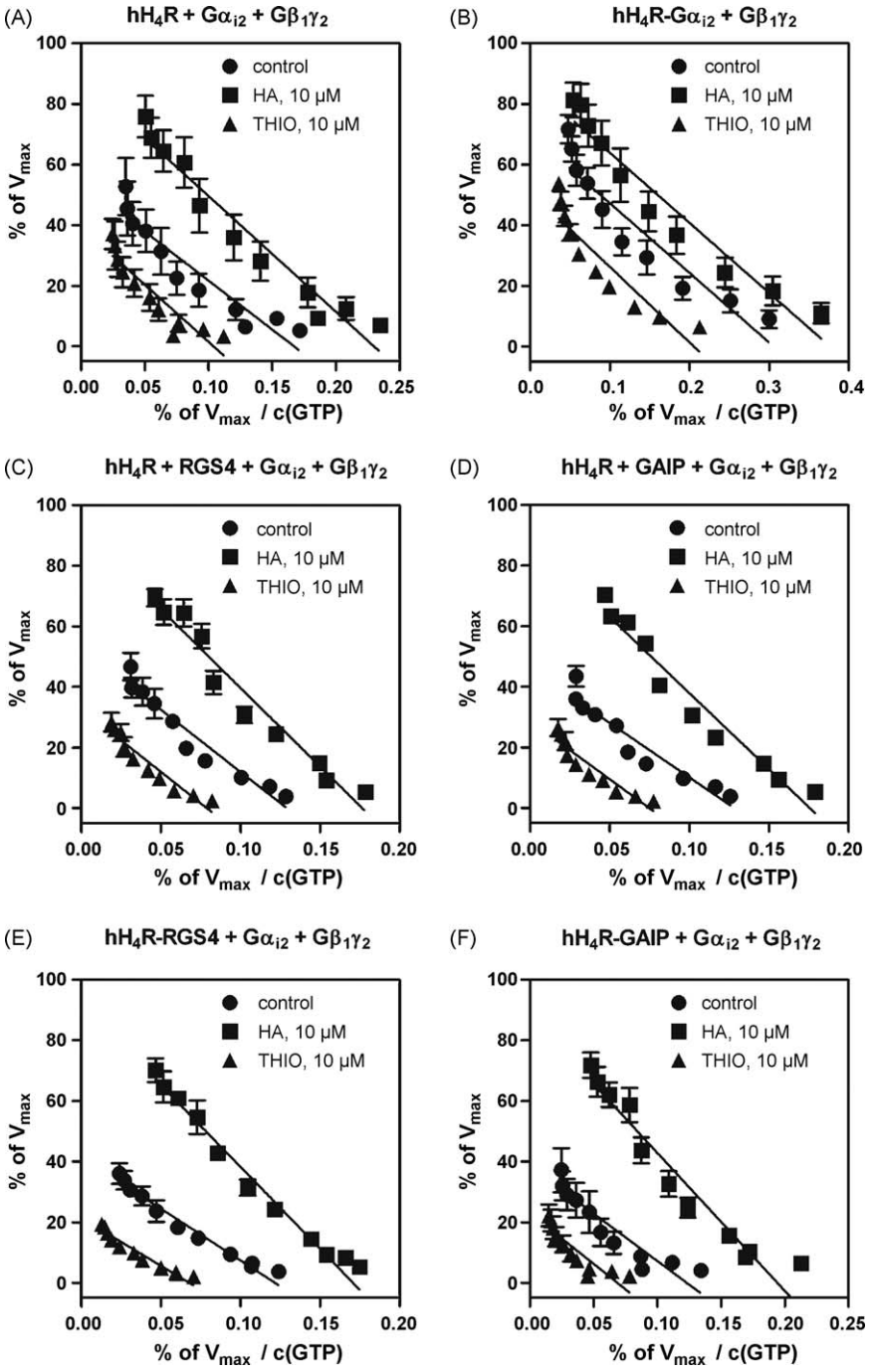

Fig. 2. Eadie–Hofstee plots, showing the effects of fused and co-expressed RGS proteins on $G\alpha_{i2}$ GTPase enzyme kinetics. Due to the large inter-membrane and inter-experimental variability of the absolute signals (cf. Table 2), all GTPase activities were related to the V_{max} value in the presence of 10 µM of HA (% of V_{max} (HA)). All data were obtained from steady-state GTPase assays in Sf9 cell membranes, co-expressing the proteins given in the title of each panel. The data for hH_4R–$G\alpha_{i2}$ were taken from a previous publication [14]. The panels show the constitutive activity (●) as well as the effect of HA (■) and THIO (▲). HA and THIO were used at a concentration of 10 µM each. All data shown are mean ± SD of 3–7 experiments performed in triplicates with membranes from at least two different preparations. All experiments were performed as described in Section 2.

3.6. Na^+ sensitivity of the hH_4R–GAIP fusion protein

According to the two-state model of receptor activation [15,41], GPCRs exist in an equilibrium of an active G-protein coupling conformation (R*) and an uncoupled inactive state (R). R* promotes GDP/GTP exchange at the Gα subunit and shows a higher affinity for agonists than R. Thus, agonists activate the receptor by stabilizing an R* state. Neutral antagonists bind to R and R* states with the same affinity and do not alter the equilibrium. Some receptor molecules, e.g. the hH_4R, spontaneously adopt the R* state and promote G-protein signaling in the absence of agonists, which is referred to as constitutive activity. Inverse agonists bind preferentially to the R-state and reduce the basal activity. Na^+ stabilizes the inactive R-state of many GPCRs and reduces the basal activity. This was described, e.g. for the formyl peptide receptor clone 26 and the α_2-adrenergic receptor [42,43].

In all systems described in this paper, the constitutive activity of the hH_4R was resistant to NaCl, independent of the presence of RGS proteins. All steady-state GTPase assays with the co-expression systems as well as with hH_4R–RGS4 and hH_4R–GAIP were

Table 3
Potency and efficacy of various hH_4R standard ligands at the hH_4R and at the hH_4R–RGS4 and hH_4R–GAIP fusion proteins. All results were determined in steady-state GTPase assays using Sf9 cell membranes that co-expressed the proteins given in the table. The data for the wild-type hH_4R were taken from a previous publication [14]. All data are shown as mean ± SD from 2 to 11 experiments performed in triplicates. The results from the hH_4R–RGS fusion proteins were compared to the data obtained from the wild-type hH_4R in one-way ANOVA, followed by Dunnet's multiple comparison test (significant difference: $^*p < 0.05$). All experiments were performed as described under Section 2.

Ligand	$hH_4R + G\alpha_{i2} + G\beta_1\gamma_2$		hH_4R–RGS4 + $G\alpha_{i2} + G\beta_1\gamma_2$		hH_4R–GAIP + $G\alpha_{i2} + G\beta_1\gamma_2$	
	EC_{50} (nM)	Efficacy	EC_{50} (nM)	Efficacy	EC_{50} (nM)	Efficacy
Histamine	13 ± 6	1.00	21 ± 7*	1.00	13 ± 7	1.00
Imetit	7 ± 5	0.69 ± 0.15	13 ± 7	0.62 ± 0.03	16 ± 4	0.75 ± 0.18
Immepip	44 ± 14	0.68 ± 0.15	85 ± 61	0.67 ± 0.14	12 ± 3	0.88 ± 0.24
R-α-methylhistamine	277 ± 96	0.92 ± 0.01	368 ± 158	0.97 ± 0.11	301 ± 35	0.83 ± 0.10
5-Methylhistamine	32 ± 8	0.87 ± 0.01	71 ± 32	1.08 ± 0.10*	35 ± 27	0.92 ± 0.08
Iodophenpropit	n.a.	~0.00	n.a.	~0.00	n.a.	~0.00
Thioperamide	96 ± 42	−1.00	179 ± 64	−1.00	65 ± 28	−1.00
JNJ-7777120	38 ± 9	−0.31 ± 0.07	91 ± 45*	−0.28 ± 0.04	32 ± 13	−0.39 ± 0.07

n.a. = neutral antagonist.

performed in the presence of 100 mM of NaCl. The effects of THIO shown in Tables 1–3 as well as in Figs. 2–4 clearly demonstrate that inverse agonism is preserved even in the presence of NaCl.

However, to completely characterize the hH_4R–GAIP fusion protein ($+G\alpha_{i2} + G\beta_1\gamma_2$) and to ensure that this new test system can fully replace the standard co-expression system with the hH_4R ($+G\alpha_{i2} + G\beta_1\gamma_2$), we also investigated the Na^+ effect for the whole range of Na^+ concentrations between 0 and 125 mM in steady-state GTPase assays. For each NaCl concentration the constitutive activity (control), the effect of HA (10 μM) and of THIO (10 μM) were determined. In Fig. 3, the results for hH_4R–GAIP are compared with the results recently published for the non-fused hH_4R [14]. Both systems behave very similar and show Na^+-resistant constitutive activity, even at Na^+ concentrations >100 mM (Fig. 3A and C). When the effects of HA and THIO are expressed as a percentage of total ligand-regulated steady-state GTPase activity (Fig. 3B and D), in both cases the relative effects of HA and THIO are around 50% in the presence of Na^+. Interestingly, compared to the non-fused hH_4R, the hH_4R–GAIP fusion protein shows a significantly (unpaired two-tailed *t*-test, $p < 0.05$) higher relative agonist signal and reduced constitutive activity in the absence of sodium. Thus, unlike the standard co-expression system with the non-fused hH_4R, the hH_4R–GAIP fusion protein could also be used for the characterization of ligands under Na^+-free conditions.

3.7. G-protein coupling specificity of the hH_4R–GAIP fusion protein

As already discussed in Section 3.3, GAIP shows selectivity for Gα proteins in the order $G\alpha_{i3} > G\alpha_{i1} > G\alpha_o \gg G\alpha_{i2}$. Thus, it is to be expected that fusion of GAIP to hH_4R alters the G-protein coupling specificity of the receptor. Therefore, we co-expressed hH_4R–GAIP with $G\alpha_{i1}$, $G\alpha_{i2}$, $G\alpha_{i3}$ and $G\alpha_o$ in combination with $G\beta_1\gamma_2$. The expression of G-proteins was determined by using an

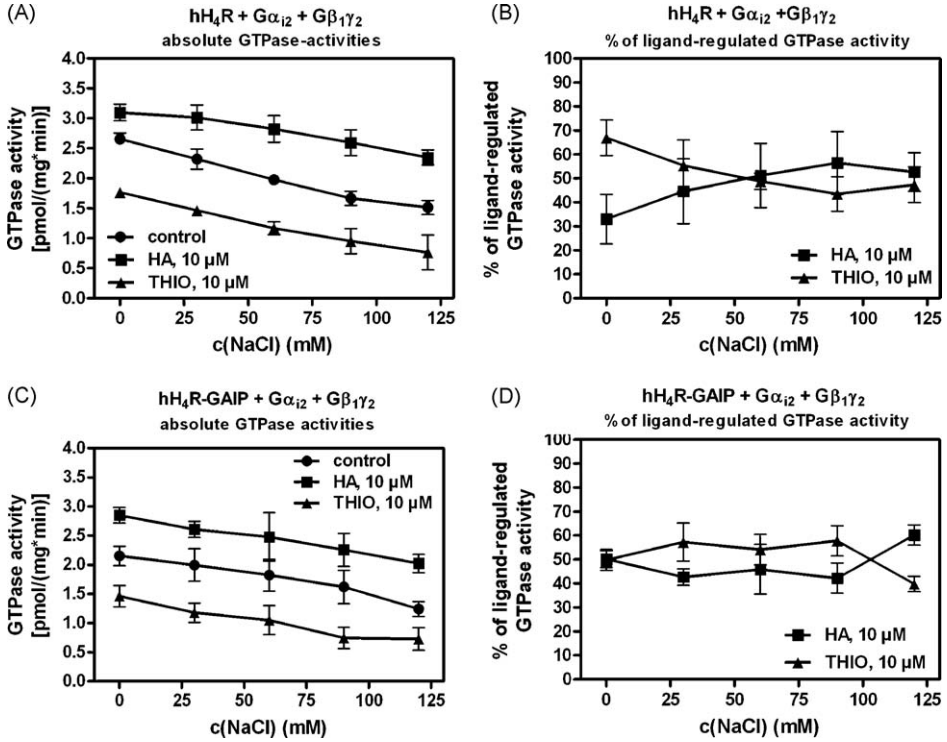

Fig. 3. Effect of NaCl on hH_4R- and hH_4R–GAIP-induced GTPase activity. Effects of NaCl on steady-state GTPase activity were studied under control conditions (●), with HA-stimulation (■) and THIO-inhibition (▲) in Sf9 cell membranes expressing hH_4R or hH_4R–GAIP with $G\alpha_{i2}$ and $G\beta_1\gamma_2$. HA and THIO were used at a concentration of 10 μM each. The GTPase assay was performed as described in Section 2. (A, C) Absolute GTPase activities in the systems expressing hH_4R (A) or hH_4R–GAIP (C). (B, D) Percentage of HA and THIO effects, related to total ligand-regulated GTPase activity, determined in the systems expressing hH_4R (B) or hH_4R–GAIP (D). Data shown are mean ± SD of three experiments performed in triplicates (one membrane preparation). The data for the non-fused hH_4R were taken from Ref. [14].

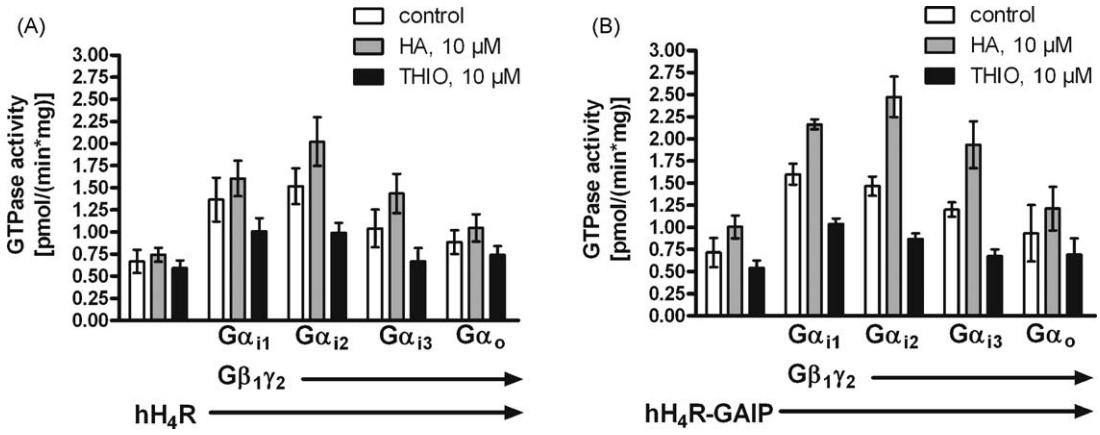

Fig. 4. Comparison of the coupling efficiency of hH_4R and hH_4R–GAIP to G-protein subtypes of the $G\alpha_{i/o}$ class. Both hH_4R (A) and hH_4R–GAIP (B) were co-expressed with $G\beta_1\gamma_2$ and various G-protein subunits of the $G\alpha_{i/o}$ class ($G\alpha_{i1}$, $G\alpha_{i2}$, $G\alpha_{i3}$ and $G\alpha_o$). As a control, hH_4R and hH_4R–GAIP were expressed in the absence of mammalian G-proteins. G-protein coupling efficiency was determined by steady-state GTPase assay. Every group of three bars in the diagram represents the results for one specific membrane under control conditions (open bar), in the presence of agonist (HA, 10 µM, grey bar) and in the presence of inverse agonist (THIO, 10 µM, black bar). The proteins expressed in the different membranes are shown below the diagram. The data represent mean ± SD of two independent assays (one membrane batch, 3–4 replicates). The data for the non-fused hH_4R were taken from Ref. [14].

anti-$G_i\alpha_{common}$ and an anti-$G\alpha_o$ antibody (data not shown). To assess the background signal, the hH_4R was also expressed without mammalian G-proteins. We determined the constitutive activity and the effects of HA (10 µM) or THIO (10 µM) in the steady-state GTPase assay. The results are shown in Fig. 4B and compared with the previously reported data for the non-fused hH_4R (Fig. 4A). Both data sets were determined with membranes prepared at the same day under the same conditions.

Surprisingly, the G-protein specificity profile of hH_4R–GAIP (Fig. 4B) was very similar to the profile of the non-fused hH_4R (Fig. 4A). Specifically, considering the HA signal there was a clear preference of hH_4R–GAIP for $G\alpha_{i2}$. Thus, the G-protein specificity of hH_4R–GAIP is governed by the properties of the GPCR, whereas the GAIP part just interacts with the Gα subunit that is bound by the receptor.

Moreover, Fig. 4 clearly demonstrates that hH_4R–GAIP shows a significantly higher relative HA-stimulation than the non-fused hH_4R when co-expressed with $G\alpha_{i1}$ or $G\alpha_{i2}$ (unpaired two-tailed *t*-test, $p < 0.05$). In the presence of $G\alpha_{i3}$ and $G\alpha_o$ the difference between the relative HA signal induced at hH_4R and hH_4R–GAIP did not reach significance. When hH_4R was expressed without mammalian G-proteins, there was a very weak HA-induced stimulation of GTPase activity (Fig. 4A, first triplet of bars). Interestingly, this stimulation was markedly increased with hH_4R–GAIP (Fig. 4B, first triplet). Most likely, this is a weak but hardly productive interaction of hH_4R with insect cell G-proteins that becomes unmasked in the presence of GAIP. Since RGS proteins do not interact with $G\alpha_s$, the observed interaction can only be due to $G\alpha_q$- or $G\alpha_i$-like proteins that both are present in Sf9 cells [44]. We previously observed a similar effect, when hH_1R or gpH_1R were co-expressed with the regulators of G-protein signaling RGS4 and GAIP in Sf9 cell membranes [27].

3.8. Conclusion

Compared to the standard system ($hH_4R + G\alpha_{i2} + G\beta_1\gamma_2$), co-expression of the hH_4R–GAIP fusion protein with $G\alpha_{i2}$ and $G\beta_1\gamma_2$ resulted in an increase of both the relative agonist-stimulated and inverse agonist-inhibited signal. Compared to the non-fused hH_4R, the hH_4R–GAIP fusion protein shows unchanged G-protein selectivity. The NaCl insensitivity of the R-state, which was previously reported for the hH_4R [14], was retained with the hH_4R–GAIP fusion protein. With respect to the pharmacological properties of several standard ligands, hH_4R–GAIP did not significantly differ from the non-fused hH_4R. Thus, hH_4R–GAIP, co-expressed with $G\alpha_{i2}$ and $G\beta_1\gamma_2$, turned out to be a very sensitive test system for the screening of potential hH_4R ligands and can readily replace the standard co-expression system ($hH_4R + G\alpha_{i2} + G\beta_1\gamma_2$) in steady-state GTPase assays.

Acknowledgements

We would like to thank Mrs. Gertraud Wilberg and Mrs. Astrid Seefeld for their excellent technical assistance. Thanks are also due to the reviewers for their helpful critique. This work was supported by the Research Training Program (Graduiertenkolleg) GRK 760 "Medicinal Chemistry–Ligand-Receptor Interactions" of the Deutsche Forschungsgemeinschaft (DFG).

References

[1] Hill SJ, Ganellin CR, Timmerman H, Schwartz JC, Shankley NP, Young JM, et al. International Union of Pharmacology XIII. Classification of histamine receptors. Pharmacol Rev 1997;49:253–78.
[2] Raible DG, Lenahan T, Fayvilevich Y, Kosinski R, Schulman ES. Pharmacologic characterization of a novel histamine receptor on human eosinophils. Am J Respir Crit Care Med 1994;149:1506–11.
[3] Oda T, Morikawa N, Saito Y, Masuho Y, Matsumoto S. Molecular cloning and characterization of a novel type of histamine receptor preferentially expressed in leukocytes. J Biol Chem 2000;275:36781–6.
[4] Morse KL, Behan J, Laz TM, West Jr RE, Greenfeder SA, Anthes JC, et al. Cloning and characterization of a novel human histamine receptor. J Pharmacol Exp Ther 2001;296:1058–66.
[5] Liu C, Ma X, Jiang X, Wilson SJ, Hofstra CL, Blevitt J, et al. Cloning and pharmacological characterization of a fourth histamine receptor (H_4) expressed in bone marrow. Mol Pharmacol 2001;59:420–6.
[6] Nakamura T, Itadani H, Hidaka Y, Ohta M, Tanaka K. Molecular cloning and characterization of a new human histamine receptor HH_4R. Biochem Biophys Res Commun 2000;279:615–20.
[7] O'Reilly M, Alpert R, Jenkinson S, Gladue RP, Foo S, Trim S, et al. Identification of a histamine H_4 receptor on human eosinophils—role in eosinophil chemotaxis. J Recept Signal Transduct Res 2002;22:431–48.
[8] Hofstra CL, Desai PJ, Thurmond RL, Fung-Leung WP. Histamine H_4 receptor mediates chemotaxis and calcium mobilization of mast cells. J Pharmacol Exp Ther 2003;305:1212–21.
[9] Strakhova MI, Nikkel AL, Manelli AM, Hsieh GC, Esbenshade TA, Brioni JD, et al. Localization of histamine H_4 receptors in the central nervous system of human and rat. Brain Res 2009;1250:41–8.
[10] Dunford PJ, Williams KN, Desai PJ, Karlsson L, McQueen D, Thurmond RL. Histamine H_4 receptor antagonists are superior to traditional antihistamines in the attenuation of experimental pruritus. J Allergy Clin Immunol 2007; 119:176–83.

[11] Varga C, Horvath K, Berko A, Thurmond RL, Dunford PJ, Whittle BJ. Inhibitory effects of histamine H_4 receptor antagonists on experimental colitis in the rat. Eur J Pharmacol 2005;522:130–8.
[12] Dunford PJ, O'Donnell N, Riley JP, Williams KN, Karlsson L, Thurmond RL. The histamine H_4 receptor mediates allergic airway inflammation by regulating the activation of $CD4^+$ T cells. J Immunol 2006;176:7062–70.
[13] Alousi AA, Jasper JR, Insel PA, Motulsky HJ. Stoichiometry of receptor-G_s-adenylate cyclase interactions. FASEB J 1991;5:2300–3.
[14] Schneider EH, Schnell D, Papa D, Seifert R. High constitutive activity and a G-protein-independent high-affinity state of the human histamine H_4-receptor. Biochemistry 2009;48:1424–38.
[15] Seifert R, Wenzel-Seifert K. Constitutive activity of G-protein-coupled receptors: cause of disease and common property of wild-type receptors. Naunyn Schmiedebergs Arch Pharmacol 2002;366:381–416.
[16] Seifert R, Wenzel-Seifert K, Kobilka BK. GPCR-Gα fusion proteins: molecular analysis of receptor-G-protein coupling. Trends Pharmacol Sci 1999;20:383–9.
[17] Wenzel-Seifert K, Hurt CM, Seifert R. High constitutive activity of the human formyl peptide receptor. J Biol Chem 1998;273:24181–9.
[18] Kleemann P, Papa D, Vigil-Cruz S, Seifert R. Functional reconstitution of the human chemokine receptor CXCR4 with G_i/G_o-proteins in Sf9 insect cells. Naunyn Schmiedebergs Arch Pharmacol 2008;378:261–74.
[19] Nickl K, Gardner EE, Geiger S, Heilmann J, Seifert R. Differential coupling of the human cannabinoid receptors hCB_1R and hCB_2R to the G-protein $G\alpha_{i2}\beta_1\gamma_2$. Neurosci Lett 2008;447:68–72.
[20] Willars GB. Mammalian RGS proteins: multifunctional regulators of cellular signalling. Semin Cell Dev Biol 2006;17:363–76.
[21] Bahia DS, Sartania N, Ward RJ, Cavalli A, Jones TL, Druey KM, et al. Concerted stimulation and deactivation of pertussis toxin-sensitive G proteins by chimeric G protein-coupled receptor-regulator of G protein signaling 4 fusion proteins: analysis of the contribution of palmitoylated cysteine residues to the GAP activity of RGS4. J Neurochem 2003;85:1289–98.
[22] Berman DM, Kozasa T, Gilman AG. The GTPase-activating protein RGS4 stabilizes the transition state for nucleotide hydrolysis. J Biol Chem 1996;271:27209–12.
[23] Cavalli A, Druey KM, Milligan G. The regulator of G protein signaling RGS4 selectively enhances α_{2A}-adreoreceptor stimulation of the GTPase activity of $Go_1\alpha$ and $G_{i2}\alpha$. J Biol Chem 2000;275:23693–9.
[24] Xu X, Zeng W, Popov S, Berman DM, Davignon I, Yu K, et al. RGS proteins determine signaling specificity of G_q-coupled receptors. J Biol Chem 1999;274:3549–56.
[25] Wieland T, Mittmann C. Regulators of G-protein signalling: multifunctional proteins with impact on signalling in the cardiovascular system. Pharmacol Ther 2003;97:95–115.
[26] De Vries L, Elenko E, Hubler L, Jones TL, Farquhar MG. GAIP is membrane-anchored by palmitoylation and interacts with the activated (GTP-bound) form of $G\alpha_i$ subunits. Proc Natl Acad Sci U S A 1996;93:15203–8.
[27] Houston C, Wenzel-Seifert K, Bürckstümmer T, Seifert R. The human histamine H_2-receptor couples more efficiently to Sf9 insect cell G_s-proteins than to insect cell G_q-proteins: limitations of Sf9 cells for the analysis of receptor/G_q-protein coupling. J Neurochem 2002;80:678–96.
[28] Walseth TF, Johnson RA. The enzymatic preparation of [α-^{32}P]nucleoside triphosphates, cyclic [^{32}P] AMP, and cyclic [^{32}P] GMP. Biochim Biophys Acta 1979;562:11–31.
[29] Preuss H, Ghorai P, Kraus A, Dove S, Buschauer A, Seifert R. Constitutive activity and ligand selectivity of human, guinea pig, rat, and canine histamine H_2 receptors. J Pharmacol Exp Ther 2007;321:983–95.
[30] Gether U, Lin S, Kobilka BK. Fluorescent labeling of purified β_2 adrenergic receptor. Evidence for ligand-specific conformational changes. J Biol Chem 1995;270:28268–75.
[31] van Rijn RM, Chazot PL, Shenton FC, Sansuk K, Bakker RA, Leurs R. Oligomerization of recombinant and endogenously expressed human histamine H_4 receptors. Mol Pharmacol 2006;70:604–15.
[32] Abramow-Newerly M, Roy AA, Nunn C, Chidiac P. RGS proteins have a signalling complex: interactions between RGS proteins and GPCRs, effectors, and auxiliary proteins. Cell Signal 2006;18:579–91.
[33] Benians A, Nobles M, Hosny S, Tinker A. Regulators of G-protein signaling form a quaternary complex with the agonist, receptor, and G-protein. A novel explanation for the acceleration of signaling activation kinetics. J Biol Chem 2005;280:13383–94.
[34] Zeng W, Xu X, Popov S, Mukhopadhyay S, Chidiac P, Swistok J, et al. The N-terminal domain of RGS4 confers receptor-selective inhibition of G protein signaling. J Biol Chem 1998;273:34687–90.
[35] De Vries L, Mousli M, Wurmser A, Farquhar MG. GAIP a protein that specifically interacts with the trimeric G protein $G\alpha_{i3}$, is a member of a protein family with a highly conserved core domain. Proc Natl Acad Sci U S A 1995;92:11916–20.
[36] The Universal Protein Resource (UniProt) 2009. Nucleic Acids Res 2009;37:D169–74.
[37] Wenzel-Seifert K, Seifert R. Molecular analysis of β_2-adrenoceptor coupling to G_s-, G_i-, and G_q-proteins. Mol Pharmacol 2000;58:954–66.
[38] Roy AA, Lemberg KE, Chidiac P. Recruitment of RGS2 and RGS4 to the plasma membrane by G proteins and receptors reflects functional interactions. Mol Pharmacol 2003;64:587–93.
[39] Igel P, Schneider E, Schnell D, Elz S, Seifert R, Buschauer A. N^G-acylated imidazolylpropylguanidines as potent histamine H4 receptor agonists: selectivity by variation of the N^G-substituent. J Med Chem 2009;52:2623–7.
[40] Ghorai P, Kraus A, Keller M, Götte C, Igel P, Schneider E, et al. Acylguanidines as bioisosteres of guanidines: N^G-acylated imidazolylpropylguanidines, a new class of histamine H_2 receptor agonists. J Med Chem 2008;51:7193–204.
[41] Leff P. The two-state model of receptor activation. Trends Pharmacol Sci 1995;16:89–97.
[42] Seifert R, Wenzel-Seifert K. Unmasking different constitutive activity of four chemoattractant receptors using Na^+ as universal stabilizer of the inactive (R) state. Receptors Channels 2001;7:357–69.
[43] Tian WN, Deth RC. Differences in efficacy and Na^+ sensitivity between α_{2B} and α_{2D} adrenergic receptors: implications for R and R* states. Pharmacology 2000;61:14–21.
[44] Knight PJ, Grigliatti TA. Diversity of G proteins in Lepidopteran cell lines: partial sequences of six G protein alpha subunits. Arch Insect Biochem Physiol 2004;57:142–50.